Supplementary Materials for

Identification of surface urban heat versus cool islands for arid cities depends on the choice of urban and rural definitions

Zehong Liu [a], Richen Ye [b], Qiquan Yang [c, d *], Ting Hu [a], Yue Liu [e], TC Chakraborty [f], Zhenxuan Liao [g]

[a] School of Remote Sensing and Geomatics Engineering, Nanjing University of Information Science and Technology, Nanjing 210044, China
[b] Guangzhou Urban Planning & Design Survey Research Institute Co., Guangzhou, 510060, China
[c] College of Surveying & Geo-Informatics, Tongji University, Shanghai 200092, China
[d] State Key Laboratory of Lunar and Planetary Sciences, Macau University of Science and Technology, Macau, China
[e] Guangzhou Institute of Geography, Guangdong Academy of Sciences, Guangzhou, 510070, China
[f] Pacific Northwest National Laboratory, Richland, WA, USA
[g] School of Information Engineering, Sanming University, Sanming 365004, Fujian Province, China
* Corresponding author. E-mail address: qiquanyang@tongji.edu.cn (Qiquan Yang)

This file includes:

Supplementary figures (Figures S1 to S4)

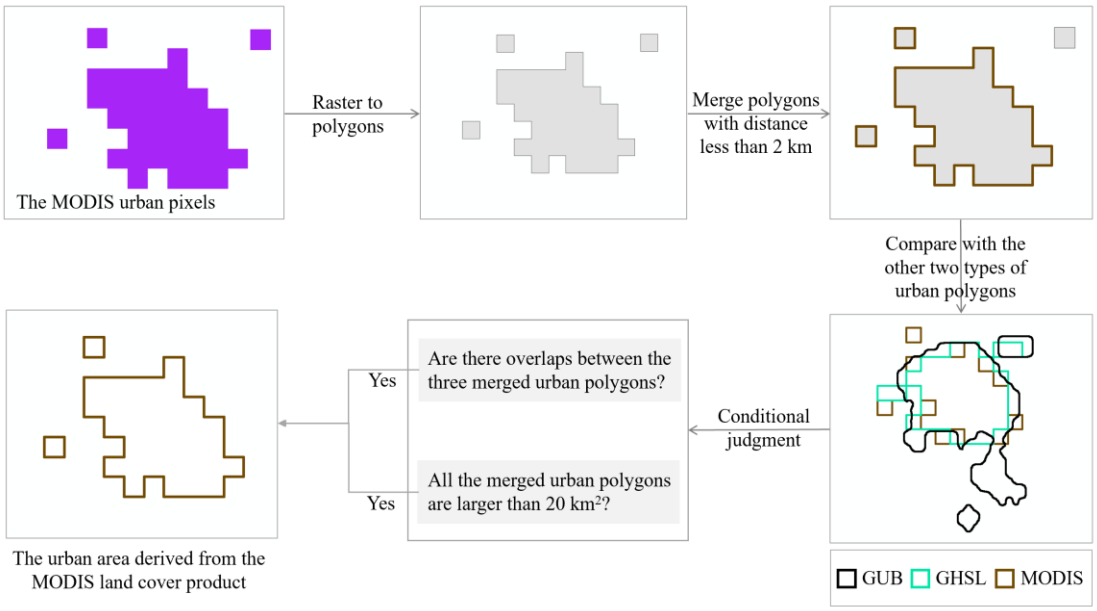

Figure S1. Flowchart for the extraction of the urban area from the MODIS land cover product. We first converted MODIS urban pixels into polygons. After that, we merged polygons that were in close proximity (less than 2 km) to each other. Then, we overlaid the merged MODIS polygons with two other sources of merged urban polygons (GUB and GHSL). Finally, the merged MODIS polygons that met the criteria were identified as the selected urban areas.

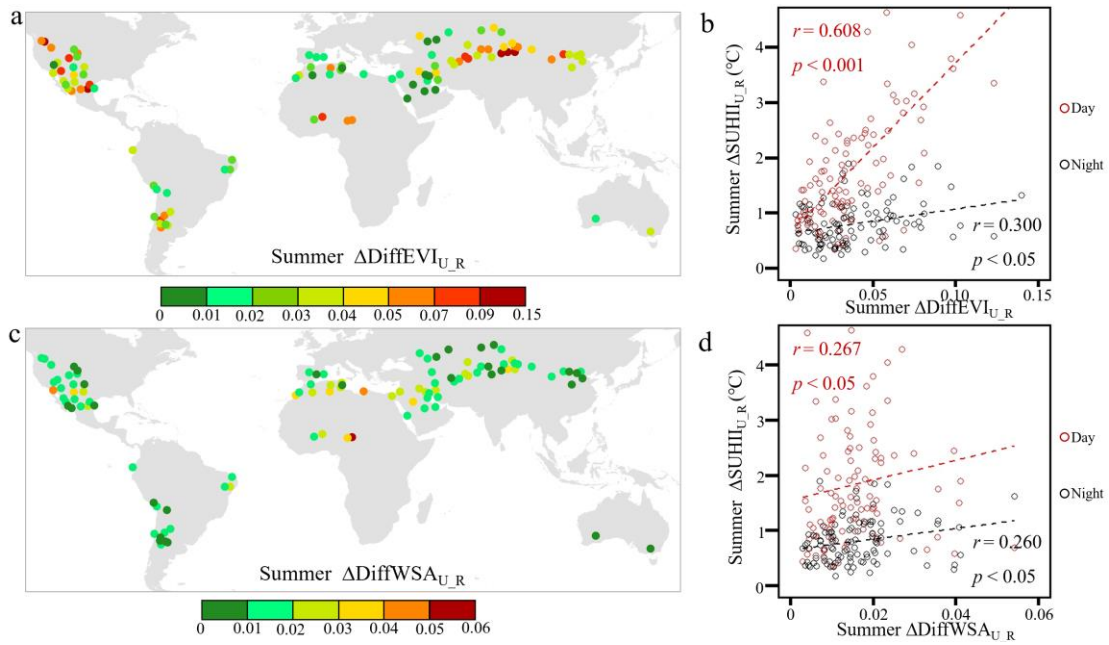

Figure S2. Spatiotemporal patterns of summer average $\Delta DiffEVI_{U\_R}$ and $\Delta DiffWSA_{U\_R}$ across global arid cities and their relationship with $\Delta SUHII_{U\_R}$. (a and c) Spatial distributions of summer average $\Delta DiffEVI_{U\_R}$ and $\Delta DiffWSA_{U\_R}$. (b) Scatterplot of summer average $\Delta SUHII_{U\_R}$ and $\Delta DiffEVI_{U\_R}$ for global arid cities. (d) Scatterplot of summer average $\Delta SUHII_{U\_R}$ and $\Delta DiffEVI_{U\_R}$ for global arid cities. The *r* represents the spearman correlation coefficient and the *p* represents the level of significance. $\Delta SUHII_{U\_R}$ refers to the SUHII uncertainty caused by co-variation of urban and rural definitions. $\Delta DiffEVI_{U\_R}$ or $\Delta DiffWSA_{U\_R}$ represents the uncertainty in urban-rural difference in EVI or WSA caused by the co-variation of urban and rural definitions.

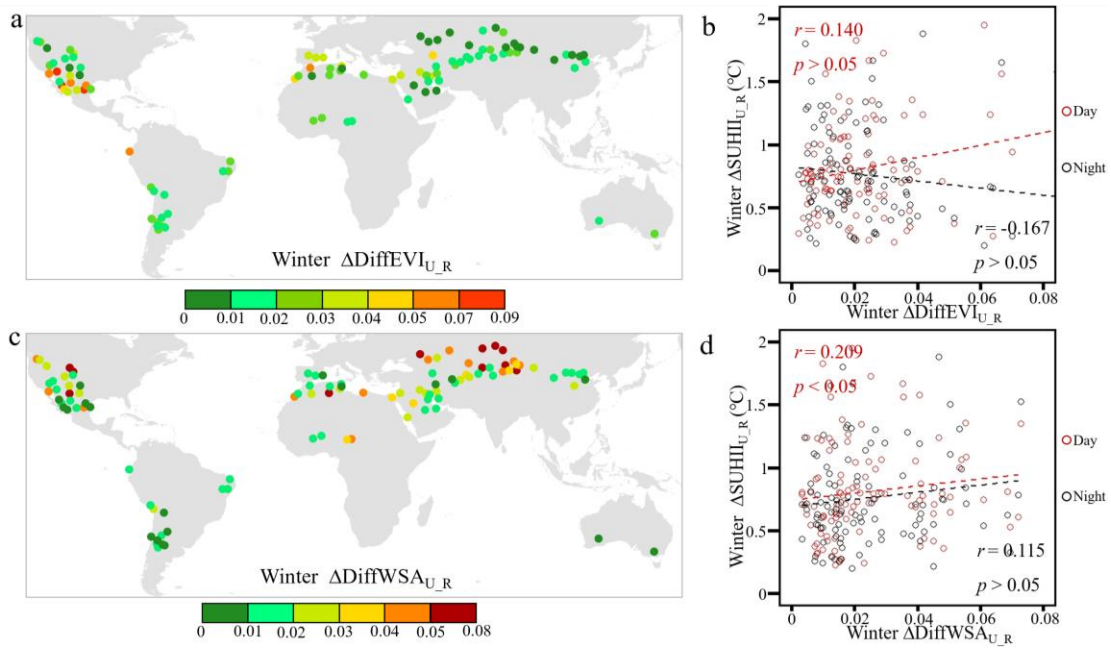

Figure S3. Spatiotemporal patterns of winter average $\Delta DiffEVI_{U\_R}$ and $\Delta DiffWSA_{U\_R}$ across global arid cities and their relationship with $\Delta SUHII_{U\_R}$. (a and c) Spatial distributions of winter average $\Delta DiffEVI_{U\_R}$ and $\Delta DiffWSA_{U\_R}$. (b) Scatterplot of winter average $\Delta SUHII_{U\_R}$ and $\Delta DiffEVI_{U\_R}$ for global arid cities. (d) Scatterplot of winter average $\Delta SUHII_{U\_R}$ and $\Delta DiffEVI_{U\_R}$ for global arid cities. The *r* represents the spearman correlation coefficient and the *p* represents the level of significance. $\Delta SUHII_{U\_R}$ refers to the SUHII uncertainty caused by co-variation of urban and rural definitions. $\Delta DiffEVI_{U\_R}$ or $\Delta DiffWSA_{U\_R}$ represents the uncertainty in urban-rural difference in EVI or WSA caused by the co-variation of urban and rural definitions.

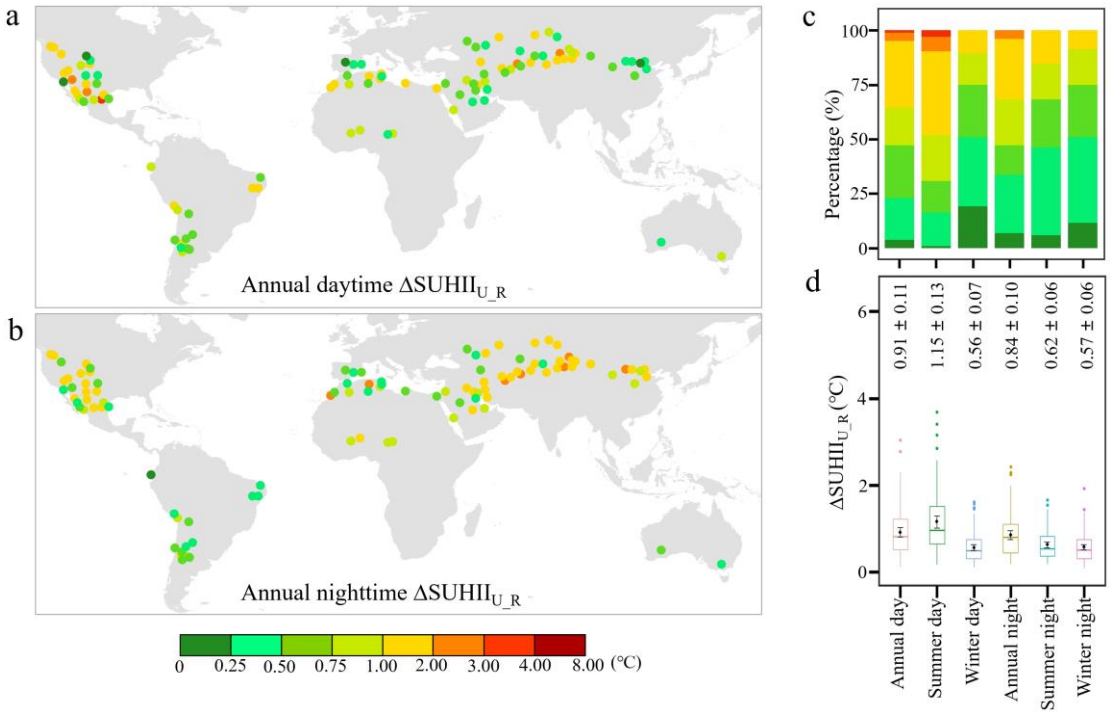

Figure S4. Spatiotemporal patterns of $\Delta SUHII_{U\_R}$ (after removing the third and fourth methods for defining rural areas) across global arid cities. (a-b) Spatial distributions of annual daytime and nighttime $\Delta SUHII_{U\_R}$. (c) Percentage-stacked bar chart of $\Delta SUHII_{U\_R}$. (d) Boxplot of $\Delta SUHII_{U\_R}$. $\Delta SUHII_{U\_R}$ represents the average absolute difference in SUHII estimates among methods with different urban and rural definitions. The central points and error bars in the boxes represent the average values and 95% confidence intervals of the $\Delta SUHII_{U\_R}$, respectively.